

CHANDRA Observations of V407 Vul: Confirmation of the Spin-up

Tod E. Strohmayer

*Laboratory for High Energy Astrophysics, NASA's Goddard Space Flight Center, Greenbelt,
MD 20771; stroh@clarence.gsfc.nasa.gov*

ABSTRACT

V407 Vul (RX J1914.4+2456) is a candidate double-degenerate binary with a putative 1.756 mHz (9.5 min) orbital frequency. In a previous timing study using archival ROSAT and ASCA data we reported evidence for an increase of this frequency at a rate consistent with expectations for gravitational radiation from a detached ultracompact binary system. Here we report the results of new *Chandra* timing observations which confirm the previous indications of spin-up of the X-ray frequency, and provide much tighter constraints on the frequency derivative, $\dot{\nu}$. We obtained with *Chandra* a total of 90 ksec of exposure in two epochs separated in time by 11.5 months. The total time span of the archival ROSAT, ASCA and new *Chandra* data is now ≈ 10.5 years. This more than doubles the interval spanned by the ROSAT and ASCA data alone, providing much greater sensitivity to a frequency derivative. With the addition of the *Chandra* data an increasing frequency is unavoidable, and the mean $\dot{\nu}$ is $7.0 \pm 0.8 \times 10^{-18}$ Hz s $^{-1}$. Although a long-term spin-up trend is confirmed, there is excess variance in the phase timing residuals, perhaps indicative of shorter timescale torque fluctuations or phase instability associated with the source of the X-ray flux. Power spectral searches for periods longward of the 9.5 minute period do not find any significant modulations, however, the sensitivity of searches in this frequency range are somewhat compromised by the dithering of the *Chandra* attitude. The observed spin-up is of a magnitude consistent with that expected from gravitational radiation decay, however, the factor of ≈ 3 variations in flux combined with the timing noise could conceivably result from accretion-induced spin-up of a white dwarf. Continued monitoring to explore correlations of torque with X-ray flux could provide a further test of this hypothesis.

Subject headings: Binaries: general - Stars: individual (RX J1914.4+2456, V407 Vul) - Stars: white dwarfs - cataclysmic variables - X-rays: stars - X-rays: binaries

1. Introduction

Ultracompact binary systems could provide a promising means to observe directly the influence of gravitational radiation on orbital evolution. Moreover, such systems would be ideal sources for detection with spaced based gravitational radiation observatories (such as the planned NASA/ESA LISA mission), opening up the possibility for detailed studies of compact interacting binaries.

In recent years a pair of candidate ultracompact systems; V407 Vul (also known as RX J1914.4+2456) and RX J0806+1527 (hereafter J0806) have been proposed. These objects were first discovered by ROSAT (Motch et al. 1996; Israel et al. 1999; Beuermann et al. 1999), and initially were suggested to be members of a “soft” class of Intermediate Polars (IPs), with the X-ray periods of 569 and 321 s, respectively, representing the putative spin periods of the accreting white dwarfs. Since their discovery extensive follow-up observations have identified the optical counterparts (Ramsay et al. 2000; Israel et al. 2002; Ramsay, Hakala & Cropper 2002). Their soft X-ray spectra, the shape of the X-ray modulation, the phasing of the X-ray and optical modulations, the lack of additional longer periods, and the lack of strong optical emission lines have all called into question their IP credentials (for a discussion see Cropper et al. 2003). However, Norton, Haswell & Wynn (2004) have argued that an IP interpretation is still plausible if the systems are stream-fed, pole-switching accretors (ie. no accretion disk), and are viewed from a nearly face-on geometry.

It was Cropper et al. (1998) who first suggested that V407 Vul might be a double-degenerate compact binary. They proposed a synchronized, magnetic accretor (polar-like) model with accretion powering the X-ray flux. A non-magnetic variant was subsequently proposed by Marsh & Steeghs (2002). In this Algol-like model, the accretion stream impacts directly onto a non-magnetic primary, and the spins are not necessarily synchronized with the orbit. An interesting alternative not requiring accretion was proposed by Wu et al. (2002). They suggested a unipolar inductor model, analogous to the Jupiter - Io system (Clarke et al. 1996). If these systems are indeed compact, and thus the observed X-ray period is the orbital period, then an important discriminating factor is the magnitude and sign of the orbital evolution. If the systems are accreting stably from degenerate donors, the expected evolution is for the orbit frequency to decrease. In a previous study we (Strohmayer 2002) used archival ROSAT and ASCA data to explore the evolution of the 1.756 mHz X-ray frequency of V407 Vul over an ≈ 5 yr time period, and found evidence for a positive frequency derivative, $\dot{\nu}$, with a magnitude consistent with simple expectations for gravitational radiation induced decay of a circular orbit. Since a measurement of the frequency evolution places severe constraints on possible models, it is crucial to confirm the initial indications of orbital decay and place tighter constraints on $\dot{\nu}$. In this paper we present the results of new *Chandra*

observations which confirm an increase in the X-ray frequency and allow us to place much tighter limits on $\dot{\nu}$. In §2 we describe the *Chandra* observations and the data extraction and analysis. In §3 we discuss our phase coherent timing study, and we show that the inclusion of the *Chandra* data conclusively indicates a positive $\dot{\nu} = 7.0 \pm 0.8 \times 10^{-18} \text{ Hz s}^{-1}$. We also discuss the flux variability of the source and excess variance (timing noise) in the phase residuals. In §4 we discuss the implications of our findings for the nature of V407 Vul. We conclude in §5 with a brief summary and goals for future observations.

2. Data Extraction

We obtained a total of ≈ 90 ksec of exposure on V407 Vul with *Chandra* in February, November, December 2003, and January, 2004. A summary of these observations is given in Table 1. We observed with ACIS-S in Continuous Clocking (CC) mode in order to mitigate the effects of pile-up. To maximize the soft photon response the aimpoint was on the backside illuminated (S3) chip. Preliminary spectral analysis shows that virtually all the source photons have energies less than 1 keV. For the purposes of our work reported here we used only < 1 keV photons. Details of the *Chandra* spectroscopy will be presented in a future paper.

To prepare the data for a precise timing analysis we first corrected the detector read out times to arrival times following the CXC analysis thread on timing with CC mode data. We then corrected the arrival times to the solar system barycenter using the CIAO tool *xbary*. We used the same source coordinates employed for analysis of the ROSAT and ASCA data (see Strohmayer 2002). This produces a set of photon arrival times in the barycentric dynamical time system (TDB). The ACIS/CC mode produces a one-dimensional “image” of the portion of the sky exposed to the detectors. A realization of this image for the February, 2003 observations is shown in Figure 1. V407 Vul is the strong peak in the “image.” We extracted only events from within the source peak for our timing study. Figure 2 shows a portion of the lightcurve produced from the source extracted events, and demonstrates that *Chandra* easily detects individual pulses from the source. We carried out this procedure on all the data and obtained a total of 29,383 *Chandra* events for our timing analysis.

3. Results

3.1. Coherent Timing Analysis

We performed our coherent timing studies using the Z_n^2 statistic. Since the method is described in our earlier paper we do not repeat all the details here (see Strohmayer 2002). As a first step we calculated two Z_3^2 power spectra. The first uses just the earlier ROSAT and ASCA data, while the second uses only the new *Chandra* data. This procedure allows us to compare the frequencies measured at two widely spaced epochs. A comparison of the two then determines the nature of any long term trend in the frequency evolution. This is perhaps the simplest possible analysis that one can do to search for a frequency change. The results are shown in Figures 3 and 4. Figure 3 shows the Z_3^2 power spectra for the two different epochs, ROSAT + ASCA (top), and *Chandra* (bottom). In each case we plot the difference, ΔZ_3^2 , between the peak value of Z_3^2 and the values at other frequencies. In the absence of a signal, the Z_3^2 statistic has noise properties given by the χ^2 distribution with $2 \times 3 = 6$ degrees of freedom (dof). The “forest” of minima in each plot results from the relatively sparse data sampling. Note, however, that for each dataset the best frequency *can* be identified unambiguously (the one with $\Delta Z_3^2 = 0$). This is crucially important, as correctly pointed out by Woudt & Warner (2004), who cautioned that frequency evolution claims for RX J0806.3+1527 and V407 Vul (see Hakala et al. 2003; Strohmayer 2003; Strohmayer 2002) might be compromised by an inability to identify the correct frequency at a given epoch. For the ROSAT + ASCA data the next-best alias peak is at $\Delta Z_3^2 \approx 1300$ from the best frequency. This is an enormously significant difference in ΔZ_3^2 . The probability that this alias could be the true frequency, compared to a frequency with a Z_3^2 value larger by 1300, is vanishingly small. The same is true for the *Chandra* data, for which the nearest alias peak has a $\Delta Z_3^2 \approx 696$. Although a smaller difference than for the ROSAT + ASCA data, the probability of this being the true frequency is still incredibly small. As an example, the probability to obtain a difference in ΔZ_3^2 of 100.0 (much smaller than the observed values) purely by chance is $< 3 \times 10^{-19}$.

Having shown that at each epoch we can unambiguously identify the correct frequency, we can now compare these two frequencies and test whether the frequency has changed. Figure 4 shows a zoom-in around the best ROSAT + ASCA (dashed) and *Chandra* (solid) frequencies, and clearly demonstrates that the frequency is higher in the *Chandra* epoch. The increase in frequency is about 2 nHz. A simple estimate of the mean frequency derivative can be obtained by simply dividing the measured frequency increase by the time interval between the mean epoch of the two datasets. This gives a value $\langle \dot{\nu} \rangle = 2 \times 10^{-9} \text{ Hz} / 7.6 \text{ yr} = 8.34 \times 10^{-18} \text{ Hz s}^{-1}$, which is consistent with the limits on $\dot{\nu}$ deduced from our earlier study as well as the more detailed analysis described below.

We next performed a coherent, phase connected timing analysis to jointly constrain ν_0 and $\dot{\nu}$. As in our previous study we carried out a grid search by calculating χ^2 at each ν_0 , $\dot{\nu}$ pair (see Strohmayer 2002 for details). The results are summarized in Figures 5, 6 and 7. Figure 5 shows two pairs of $\Delta\chi^2$ confidence contours. The large dashed contours represent the constraints derived only from the ROSAT + ASCA data, and the solid contours represent the best solution obtained with the inclusion of the new *Chandra* data. The analysis definitively favors a positive $\dot{\nu} = 7 \pm 0.8 \times 10^{-18}$ Hz s $^{-1}$. The parameters of our best timing ephemeris are given in Table 1.

Although the presence of a long term spin up trend in the data is now indisputable, the minimum χ^2 value of 390 (with 98 degrees of freedom) for our best fit is formally high. Because of this we first scaled the χ^2 values for the whole dataset (including *Chandra*) by the ratio $390/98 \approx 4$ before plotting the confidence contours. This gives a conservative estimate of the confidence region for ν and $\dot{\nu}$. Figure 6 shows two representations of the phase measurements. The phase residuals obtained with $\dot{\nu} = 0$ and our best constant frequency, ν_0 , for all the data are shown in the top panel. In this representation a positive $\dot{\nu}$ (spin-up) will show up as a quadratic trend with the parabola opening downward. One can clearly pick out such a trend with the eye. The phase residuals computed with our best ephemeris (ie. including the best non-zero value of $\dot{\nu}$) are shown in the bottom panel. Figure 7 is essentially identical to Figure 6 except the time gaps have been removed so that all the individual residuals can be more easily seen. Note the much higher statistical quality of the *Chandra* data.

The excess χ^2 value is indicative of some additional “timing noise” in the system. Although the rms deviations are qualitatively similar for all the data, the much higher statistical quality of the *Chandra* data contributes substantially to the excess. The presence of timing noise could in principle result from fluctuations in the spin up torque, or perhaps from modest changes in the profile of the pulsed emission. By monitoring the character of such fluctuations it should be possible to further constrain models for the spin up torque. We discuss this further below. Since fluctuations of both sign appear, and over a range of timescales, it seems extremely unlikely that the overall spin up trend could somehow result from a random superposition of fluctuations with just the right amplitude and phasing. Using our best timing ephemeris we have calculated folded pulse profiles for the ROSAT + ASCA and new *Chandra* data. The results are shown in Figure 8. The *Chandra* profile has been displaced vertically by 600 counts for clarity. Phase zero in the plot corresponds to MJD 49257.533373137 (TDB). The pulse profile appears to be rather stable over the past decade.

3.2. Flux Variability

An important constraint on models for V407 Vul is the present lack of any detectable periodicities with timescales longer than the 1.756 mHz X-ray modulation. If the system were in fact an IP, then one might expect that the longer, unseen orbital period could eventually be detected with sensitive observations. The *Chandra* data are sensitive enough to explore variability on timescales longer than the X-ray pulsation. We did this by computing a lightcurve using our best fit period as the time bin size. The resulting lightcurve is shown in Figure 9. In this plot we have suppressed the time gaps. Individual observations are separated by the vertical dotted lines. Epochs for each of the five observations can be found in Table 1. The data show evidence for both long term variations in the flux as well as some pulse to pulse variations. For example, the flux during our next-to-last pointing was a factor of 3 higher than in the initial pointing. The longest pointing (2nd panel from the left) shows evidence for 30 – 50% variations in the flux within a few pulse periods.

Our 35.4 ksec pointing at V407 Vul is the longest contiguous observation of the source to date. This, combined with the higher signal to noise ratio in the *Chandra* data compared with ROSAT or ASCA, allows, in principle, more sensitive searches for a putative IP orbital period. To search for periods longward of the 1.756 mHz frequency we computed Fourier power spectra of each of our observations. We do not find any robust periodicities which are present in all of our observations. In the power spectrum of the longest pointing a weak sideband structure accompanies the fundamental and first two harmonics of the 1.756 mHz frequency. The low frequency region of this power spectrum is shown in Figure 10. The strongest of these peaks are the upper sidebands to the fundamental and first harmonic peaks at 1.756 mHz and 3.512 mHz. These sidebands are separated in frequency from their parent peaks by 0.4825 mHz, and have Leahy normalized powers of 74.8 and 52.5. There also appear to be weaker lower sidebands accompanying the first and second harmonic peaks at 3.512 mHz and 5.28 mHz respectively. These lower sidebands are separated in frequency by 0.273 mHz from their respective harmonic peaks. The upper sideband frequency separation is close to, but significantly different from, twice the lower sideband separation.

Although such a sideband structure could conceivably be intrinsic to the source, and thus could suggest a longer, previously unseen period in the system, we think a more plausible explanation is that these are spurious signals most likely introduced by the dithering of the *Chandra* pointing position. *Chandra* dithers in a Lissajous pattern with different periods in the horizontal and vertical directions. For ACIS, the dither periods are 1000 and 707 seconds in the Y and Z directions, respectively. Indeed, there is a modest peak at a 1000 s period in the power spectrum of our longest observation. It seems likely that beating between the strong 1.756 mHz modulation and the dither periods could introduce sideband

modulations. Moreover, since the strength of power spectral features is proportional to the counting rate, we would expect an astrophysical signal, if robust, to produce a greater signal in our brightest observation, yet there is no evidence for the sideband structure in the observation at the highest counting rate. Based on these arguments we do not think there is yet sufficient evidence to claim detection of a longer period. Because of the systematic issues associated with dithering *Chandra*, it seems likely that XMM observations will provide more definitive results with regard to searches for an unseen orbital period in V407 Vul.

4. Implications for the Nature of V407 Vul

Our *Chandra* data definitively shows that the 1.756 mHz X-ray modulation of V407 Vul is increasing at a mean rate of $\approx 7 \times 10^{-18} \text{ Hz s}^{-1}$. This rate is consistent with what would be expected if the X-ray modulation is the orbital period of an ultracompact system and it's orbit were decaying via emission of gravitational radiation (see Strohmayer 2002). Based on the observed spin-up there would appear to be two remaining alternatives regarding the nature of the source. 1) An ultracompact but detached system powered by electrical energy, as described by Wu et al. (2002), or 2) a low-inclination IP system in which the observed X-ray modulation is effectively the white dwarf spin, and the X-ray flux and observed spin-up are accretion driven (Norton, Haswell & Wynn 2004). Other ultracompact scenarios appear to be ruled out by the observed spin-up and/or the short orbital period (see Strohmayer 2002; Cropper et al. 2003).

In the IP scenario the white dwarf accretion is stream-fed and switches from pole to pole and back again on the synodic period. An accretion disk would form if the magnetospheric radius is less than the circularization radius for the accretion stream. In order not to form a disk and for V407 Vul to be stream-fed the orbital period must satisfy $P_{orb} < 2.37 \text{ hr}$ (Norton et al. 2004). If this scenario is correct, then the secular spin up is due to accretion onto the white dwarf, and other aspects of the observations, for example, the long term flux variability and the phase timing noise, may be more easily understood in terms of variations in the mass accretion rate. This identification would also preclude the need to invoke models perceived by some as “exotic” (such as the Wu et al. (2002) electric star scenario).

However, some intriguing questions remain, for example, the soft X-ray spectrum, the absence (or at least weakness) of optical emission lines, and the infrared photometry have all been used to argue against an IP identification (see Cropper et al. 2003 for a discussion). Norton et al. (2004) have argued that the relatively high mass accretion rates, of order $10^{-9} M_{\odot} \text{ yr}^{-1}$, required for accretion to power the observed X-ray flux, as well as the nature of stream-fed accretion may mitigate most of these perceived difficulties. For example, a

highly optically thick stream may mask the emission lines, and if the accretion is “buried” in the white dwarf surface layers, then it may manifest itself with predominantly soft blackbody emission. Deeper optical spectroscopy would likely provide important new insight.

Accretion-induced spin-up should be testable with continued phase coherent monitoring. Comparison of torque fluctuations with X-ray flux (ie. mass accretion rate) could yield a signature of magnetically controlled accretion (see for example, Ghosh & Lamb 1979). Moreover, if the frequency derivative changes sign that would strongly support the IP scenario.

5. Summary

Our new *Chandra* data confirm that the 1.756 mHz X-ray frequency of RX V407 Vul is increasing at a rate of $\approx 7 \times 10^{-18}$ Hz s $^{-1}$. Although this rate is consistent with that expected from gravitational radiation losses in a detached ultracompact binary, an IP interpretation in the context of accretion onto a spinning white dwarf cannot yet be strongly ruled out.

In some ways the new *Chandra* results have only deepened the mystery surrounding V407 Vul (and by implication, its sister source, RX J0806.3+1527). After a decade of observations we still do not know the nature of the source with any certainty. However, a number of future observations could help provide the solutions. Deep pointings with XMM could probe more sensitively for an unseen orbital period, and further timing observations with *Chandra* will establish constraints on the dependence of torque fluctuations on X-ray flux. Finally, if these do not suffice to crack the mystery, a detection with a spaced-based gravitational radiation observatory (such as the NASA/ESA LISA mission) would provide definitive evidence for an ultracompact system.

We thank Richard Mushotzky, Zaven Arzoumanian, Jean Swank and Craig Markwardt for many helpful comments and discussions. We also thank the referee for his/her detailed comments on the original manuscript, that helped us to significantly improve the paper. This work made use of data obtained from the High Energy Astrophysics Science Archive Research Center (HEASARC) at Goddard Space Flight Center.

References

759

Beuermann, K., Thomas, H. -C., Reinsch, K., Schwöpe, A. D., Trümper, J. & Voges, W. 1999, A&A, 347, 47.

Clarke, J. T. et al. 1996, Science, 274, 404

Cropper, M., Ramsay, G., Wu, K. & Hakala, P. 2003, ASP Conference Series to be published in Proc. Cape Town Workshop on magnetic CVs, held Dec 2002, (astro-ph/0302240).

Cropper, M. et al. 1998, MNRAS, 293, L57

Ghosh, P. & Lamb, F. K. 1979, ApJ, 232, 259.

Hakala, P. et al. 2003, MNRAS, 343, 10L.

Israel, G. L. et al. 1999, A&A, 349, L1.

Israel, G. L. et al. 2002, A&A, 386, L13.

Kuulkers, E., Norton, A., Schwope, A. & Warner, B. 2003, in “Compact Stellar X-ray Sources,” ed. M. van der Klis & W. H. G. Lewin, (Cambridge Univ. Press: Cambridge, UK).

Marsh, T. R. & Steeghs, D. 2002, MNRAS, 331, L7

Motch, C. et al. 1996, A&A, 307, 459

Norton, A. J., Haswell, C. A. & Wynn, G. A. 2004, A&A, in press, (astro-ph/0206013)

Ramsay, G., Cropper, M., Wu, K., Mason, K. O., & Hakala, P. 2000, MNRAS, 311, 75

Ramsay, G., et al. 2002, MNRAS in press, (astro-ph/0202281)

Ramsay, G. Hakala, P. & Cropper, M. 2002, MNRAS, 332, L7.

Ritter, H. & Kolb, U. 2003,, A&A, 404, 301.

Strohmayer, T. E., 2003, ApJ, 593, 39L.

Strohmayer, T. E., 2002, ApJ, 581, 577.

Warner, B. 1995, *Cataclysmic Variable Stars*, Cambridge Univ. Press, Cambridge UK.

Warner, B. 1986, MNRAS, 219, 347.

Woudt, P. A. & Warner, B. 2003, in Proc. Cape Town Workshop on Magnetic CVs, (astro-ph/0310494).

Wu, K., Cropper, M., Ramsay, G. & Sekiguchi, K. 2002, MNRAS, 331, 221

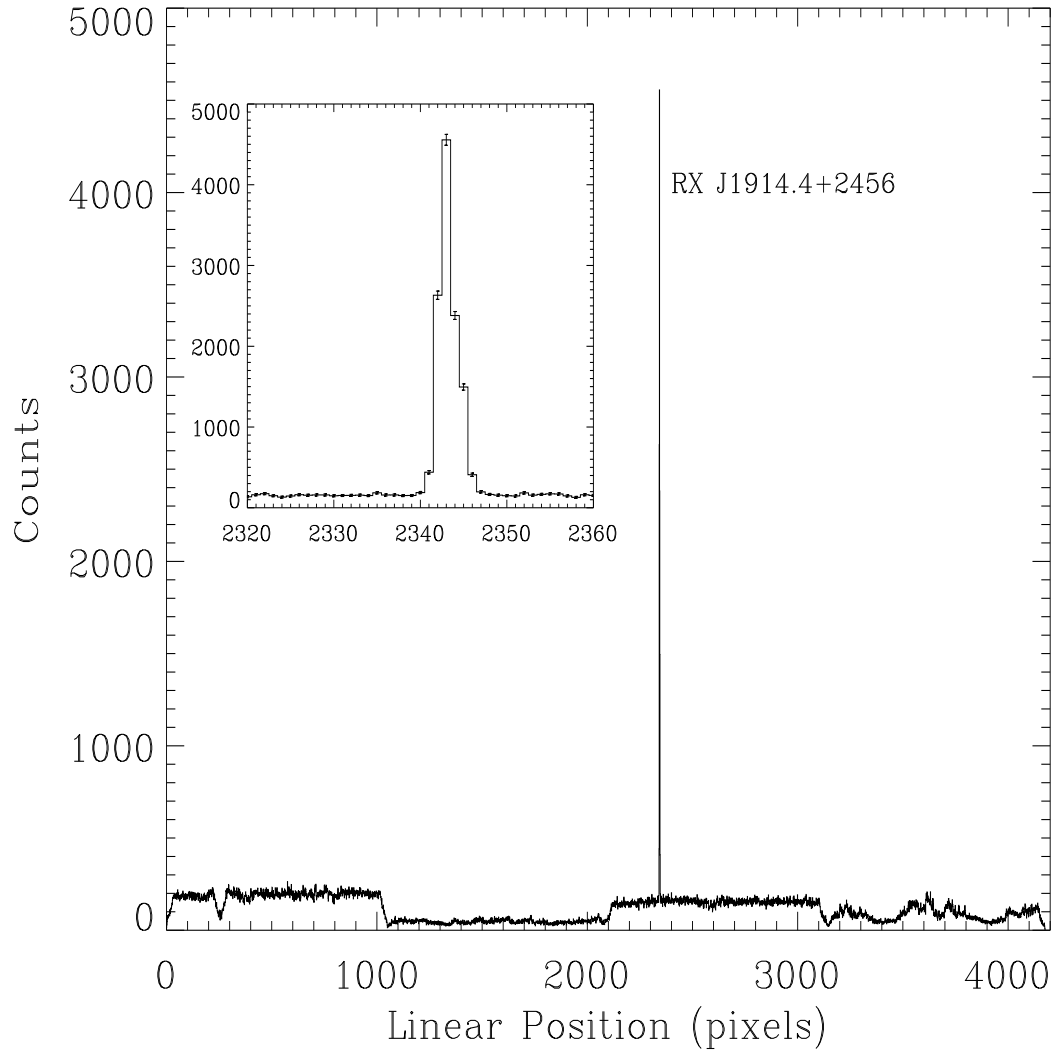


Figure 1: *Chandra* 1-d image of V407 Vul from ACIS-S Continuous Clocking mode data. The sharp peak contains photons from V407 Vul. The inset panel shows an expanded view of the peak.

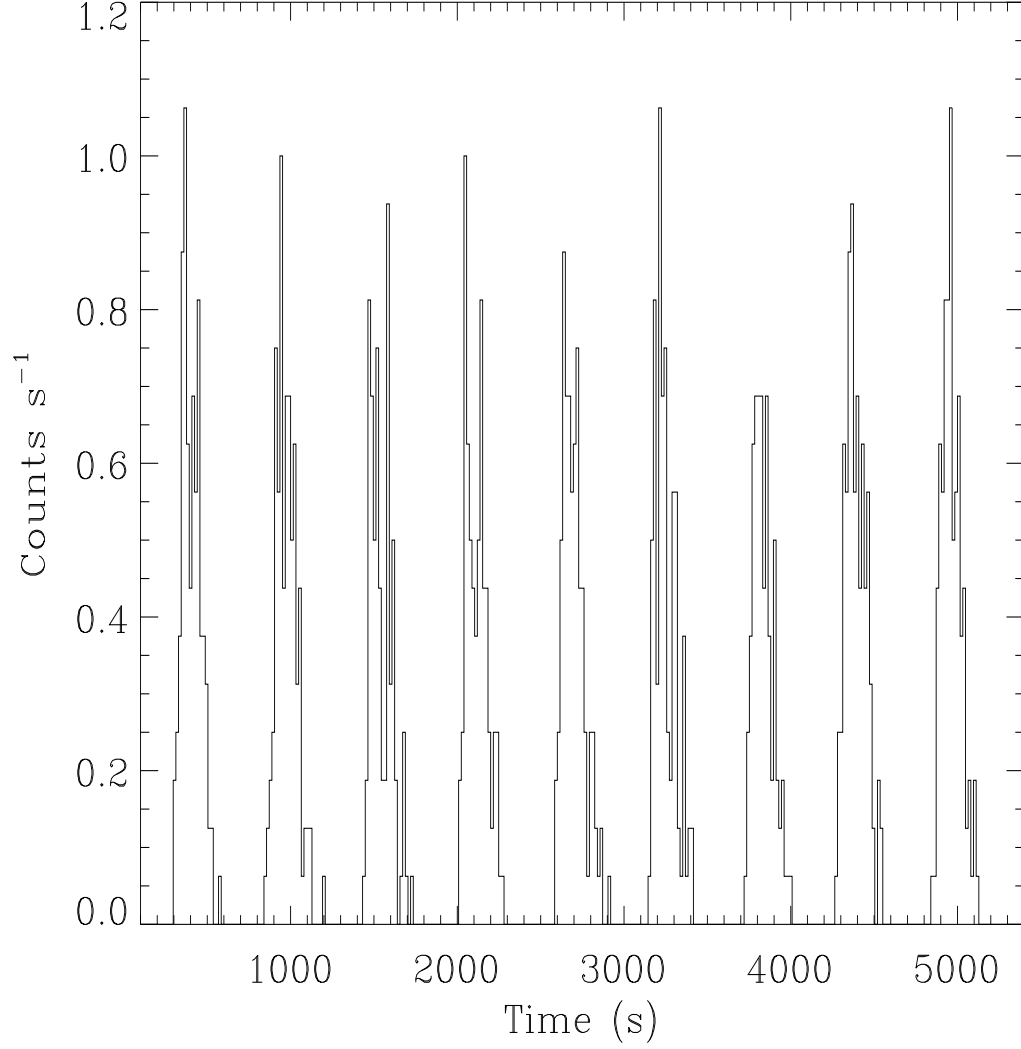


Figure 2: A lightcurve of a portion of the *Chandra* ACIS-S data from V407 Vul. The binsize is 16 s, and nine individual pulses are shown.

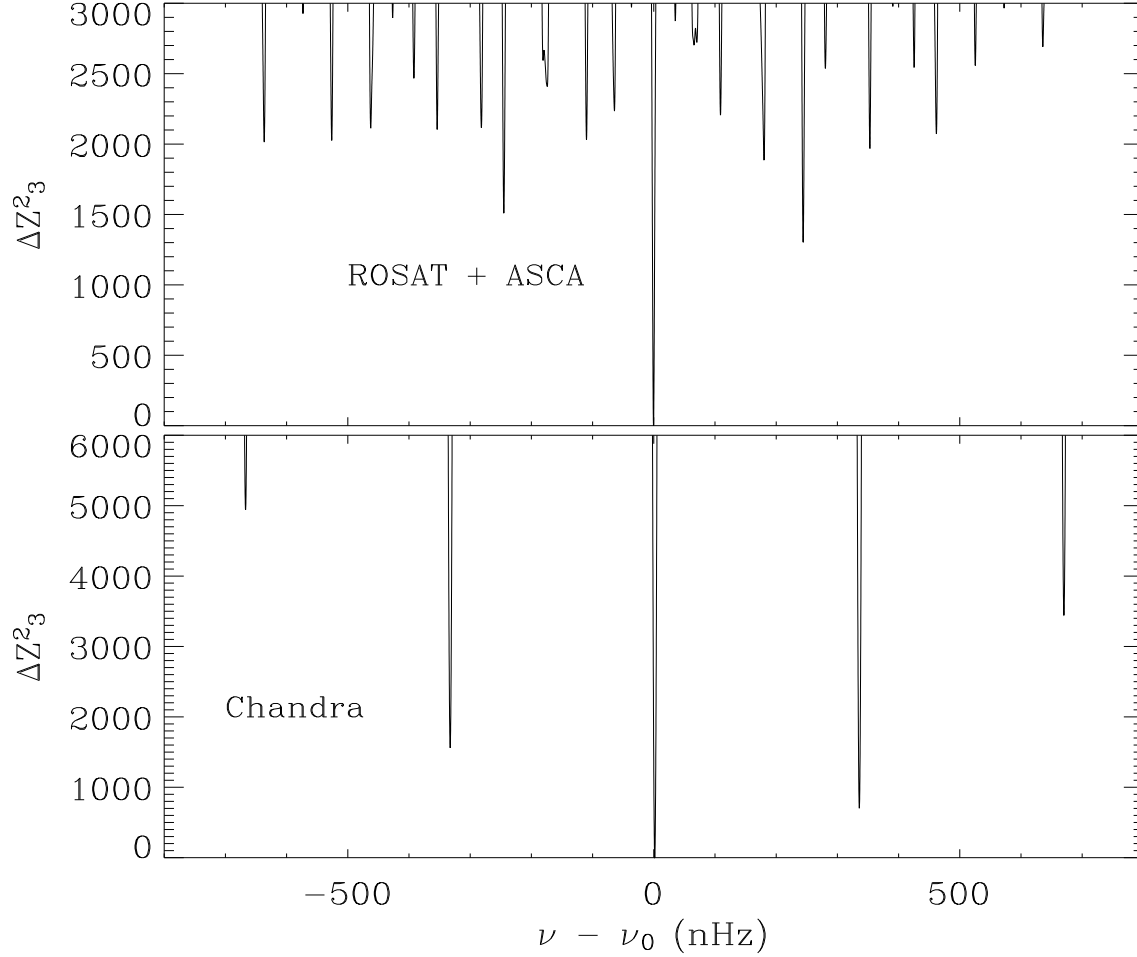


Figure 3: Best constant frequency measurements for V407 Vul at two different epochs; the combined ROSAT + ASCA data (top), and the new *Chandra* data (bottom). Shown are the values of $\Delta Z_3^2 = \max(Z_3^2) - Z_3^2$ as a function of frequency. In this representation the minima denote the best frequency values for each dataset. Multiple minima are present due to the incomplete sampling of the datasets. In each case, however, the correct frequency peak can be identified unambiguously (the peaks centered near $\nu - \nu_0 = 0$). All other peaks are at significantly high values of ΔZ_3^2 to be strongly excluded (see the text for further details). The reference frequency, ν_0 , is 1.7562475×10^{-3} Hz.

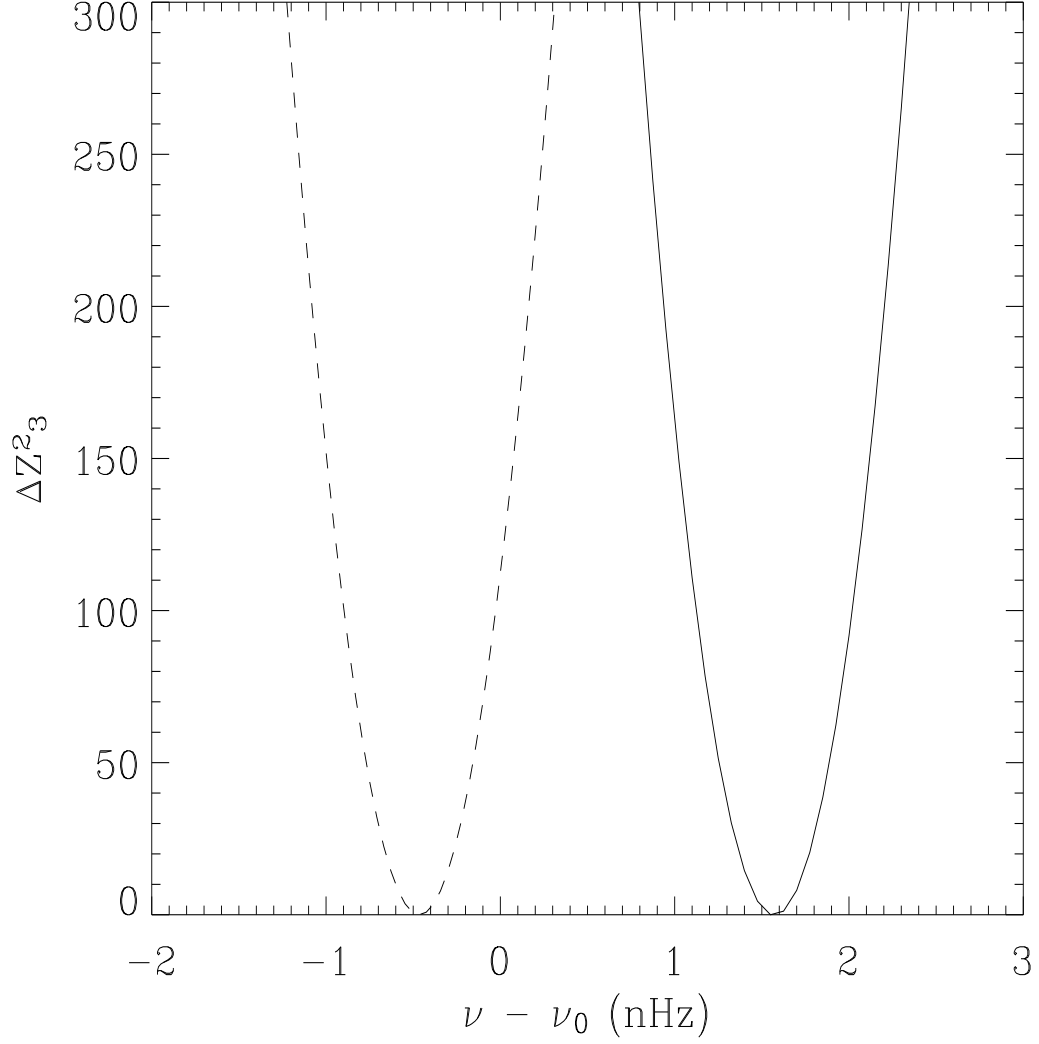


Figure 4: Same as Figure 3 but now showing an expanded view of the region around $\nu - \nu_0 = 0$. The best frequencies from the ROSAT + ASCA (dashed) and Chandra (solid) epochs are shown. The frequency measured at the more recent *Chandra* epoch is clearly higher. This establishes beyond doubt that the frequency of V407 Vul has increased over the last 11 years (see the text for further details).

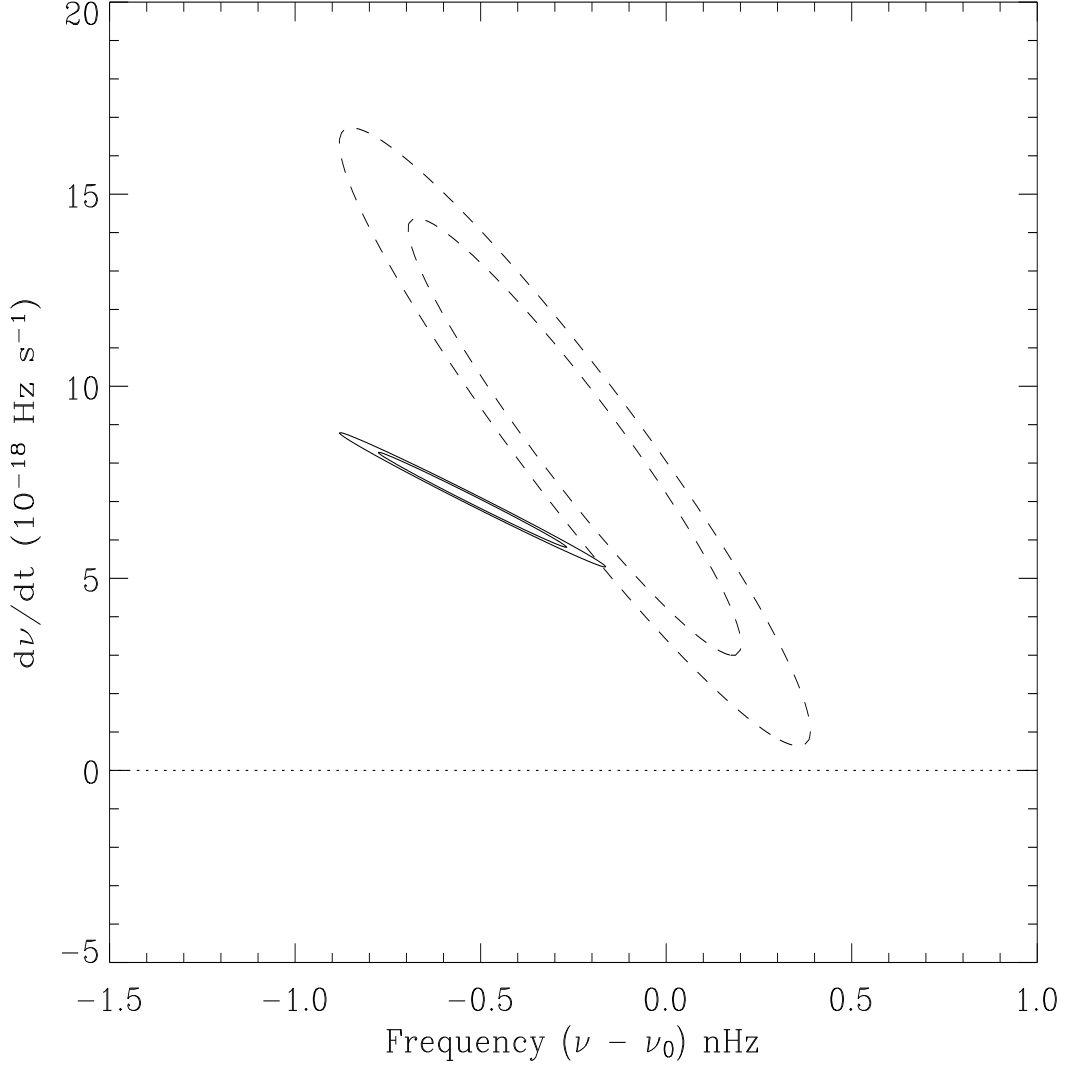


Figure 5: Constraints on ν and $\dot{\nu}$ from our phase timing analysis of the ROSAT, ASCA and new *Chandra* data for V407 Vul. Shown are the 90 and 99% confidence regions for the ROSAT + ASCA data (dashed), and the combined dataset (ROSAT, ASCA and *Chandra*). In plotting the confidence contours for all the data (solid) we first scaled the χ^2 values by the factor 390/98 (see text for discussion). The inclusion of the *Chandra* data definitively requires a positive $\dot{\nu} = 7 \pm 0.8 \times 10^{-18} \text{ Hz s}^{-1}$.

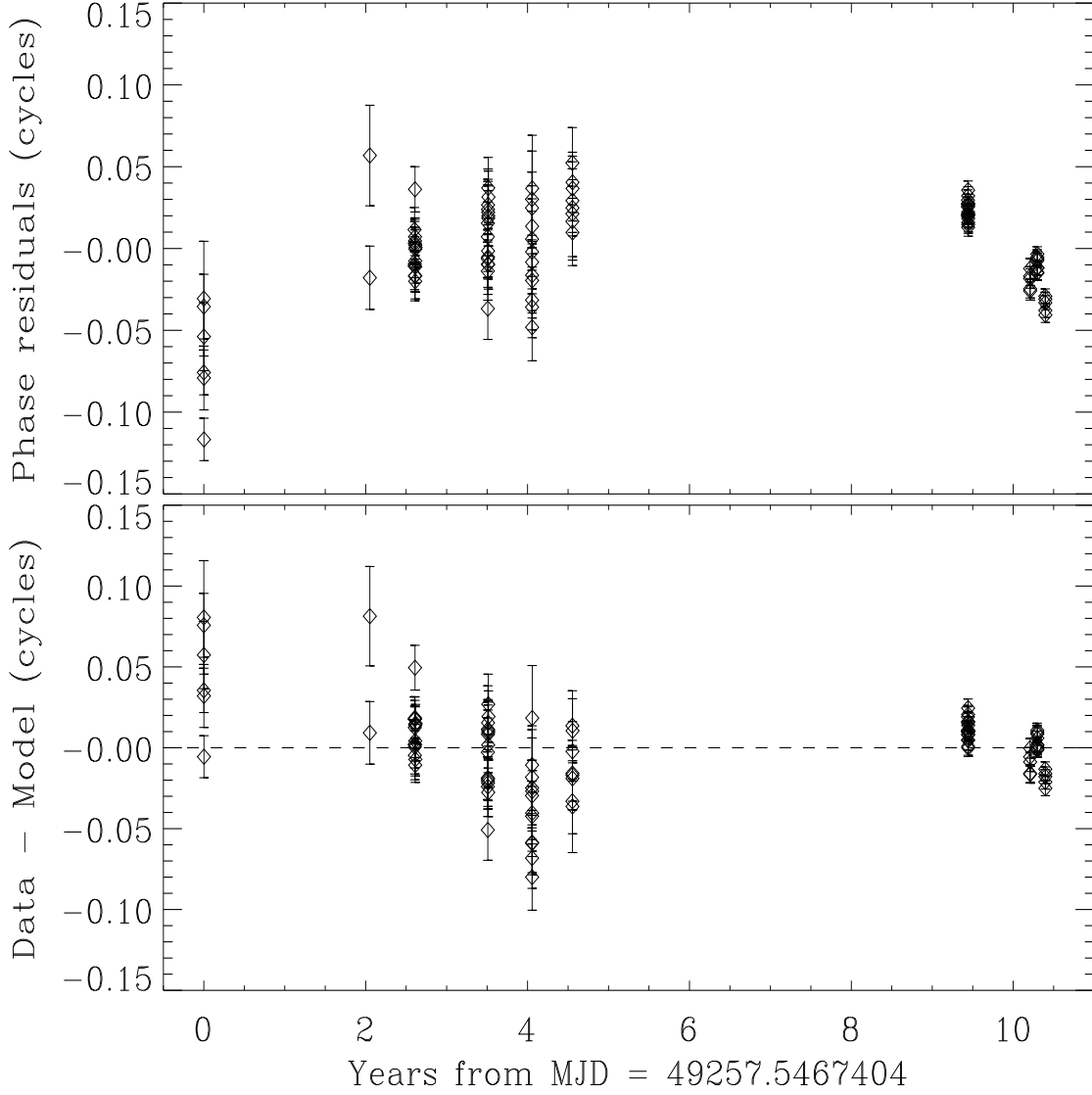


Figure 6: Phase timing residuals for V407 Vul plotted as a function of time using a constant frequency phase model (ie. $\dot{\nu} \equiv 0$ (top), and with the best fitting solution including a positive $\dot{\nu} = 7 \times 10^{-18} \text{ Hz s}^{-1}$ (bottom). In the top panel a parabolic shape with the parabola opening downward is indicative of the need for a positive $\dot{\nu}$. Such a trend can just about be discerned with the eye. The *Chandra* data are those points beyond year 9.

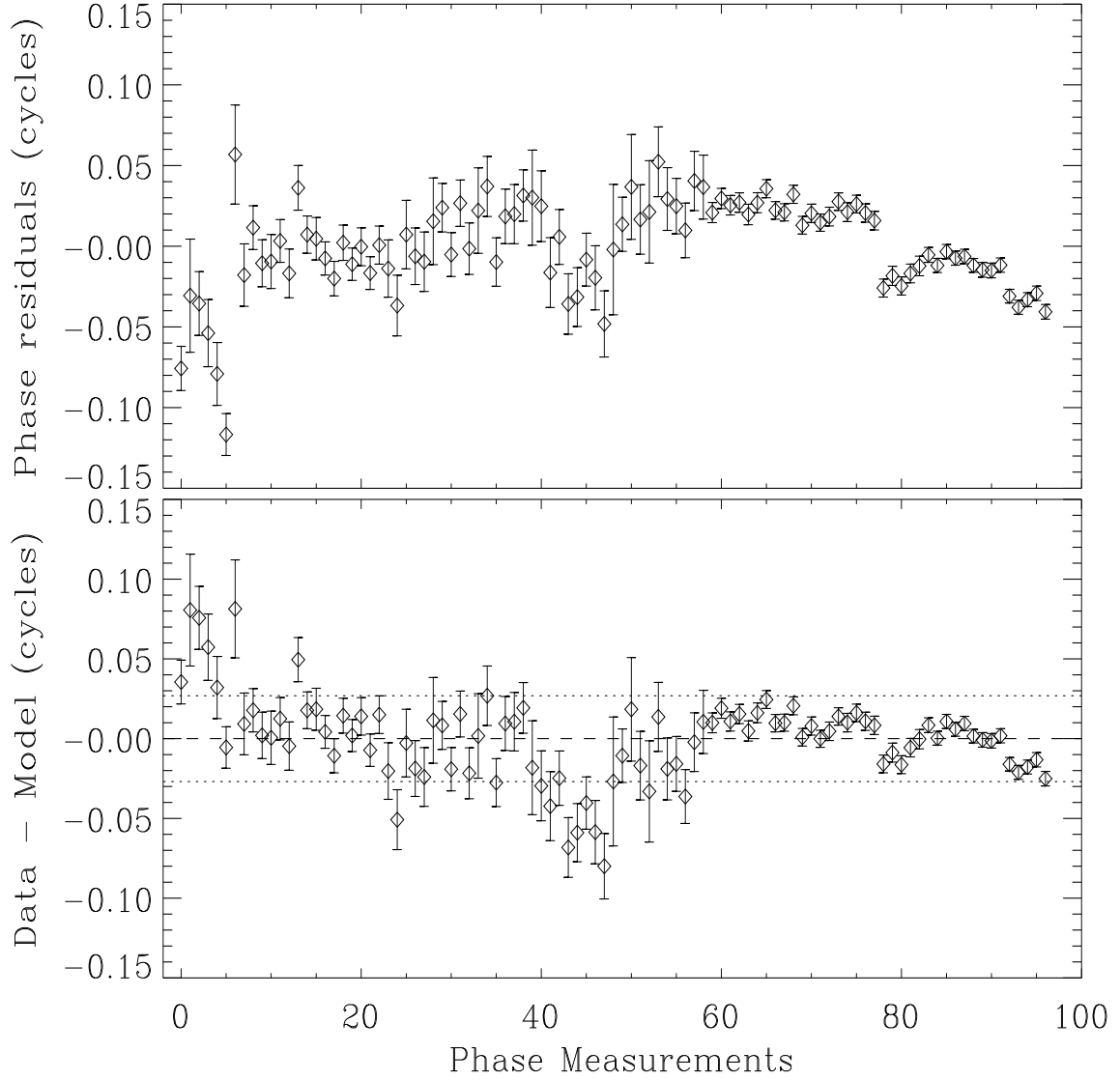


Figure 7: Same as Figure 6 except the time gaps have been removed so that the individual phase residuals can be more easily seen. The rms deviation of the residuals is also shown (dotted lines). The *Chandra* data are those beyond measurement number 58 (note the smaller error bars).

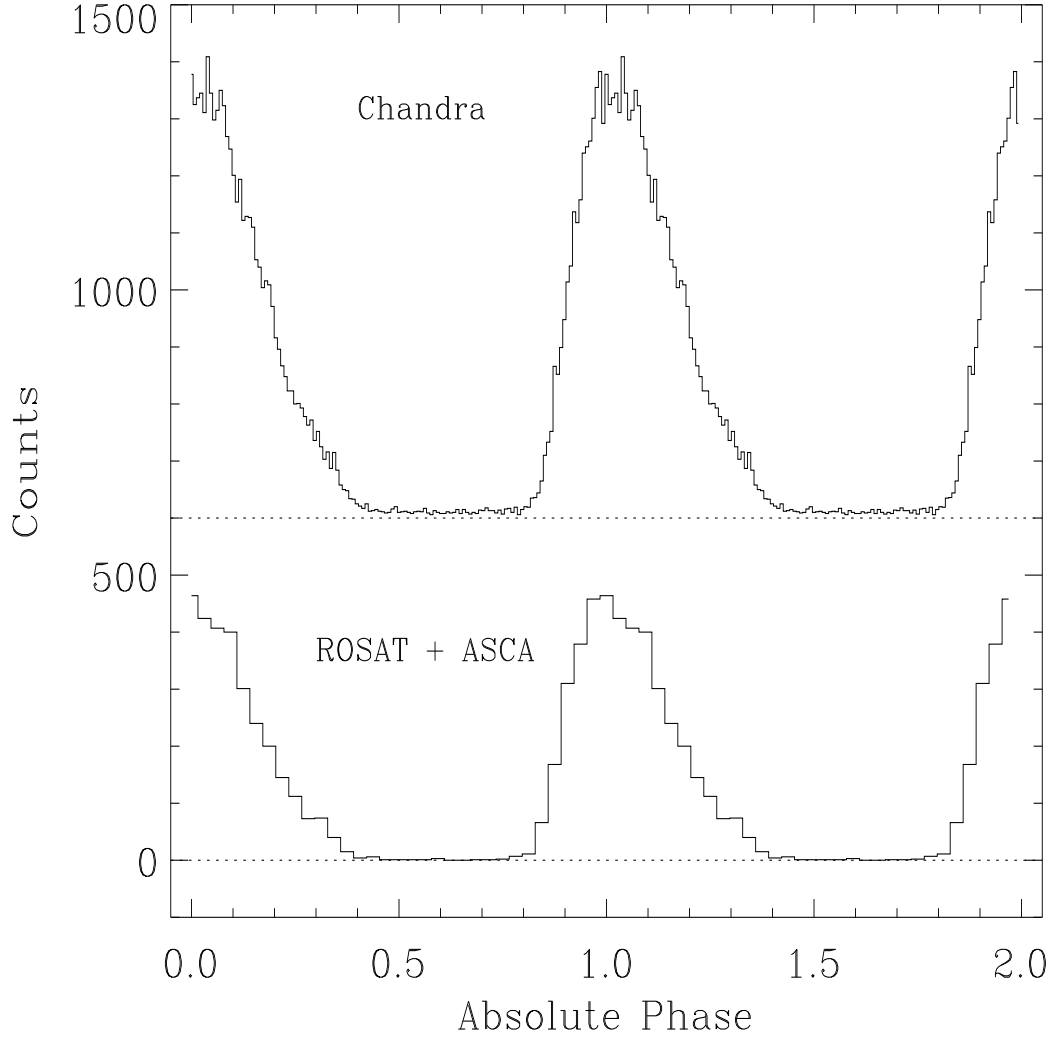


Figure 8: Folded pulse profiles for the ROSAT + ASCA (bottom) and new *Chandra* data (top) using our best timing ephemeris (see Table 1). The *Chandra* profile has been displaced vertically by 600 counts for clarity. Phase zero corresponds to MJD 49257.533373137 (TDB).

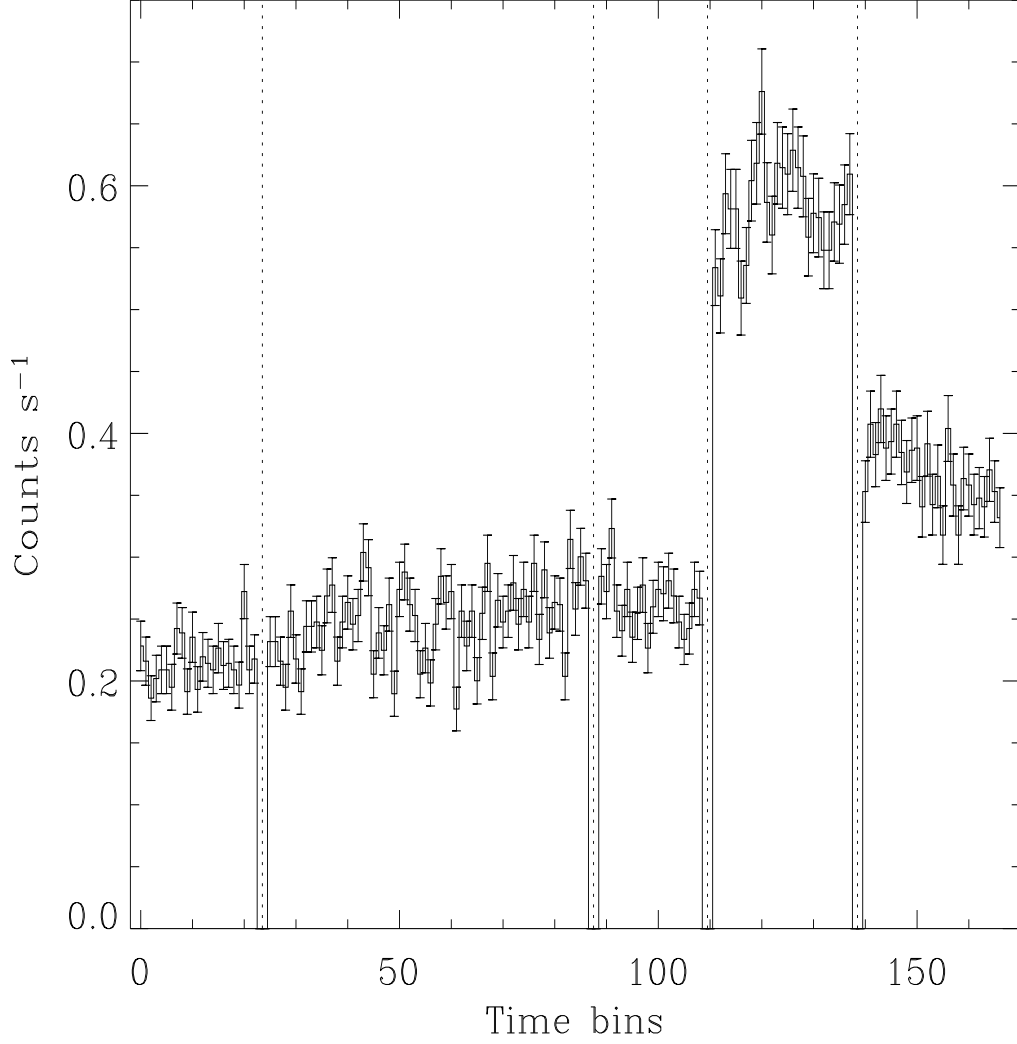


Figure 9: Flux variability of V407 Vul seen with *Chandra* at five different epochs. The time binsize was set equal to one cycle of the 1.756 mHz pulsation. There is clear evidence for large, long term flux modulations as well as shorter timescale fluctuations.

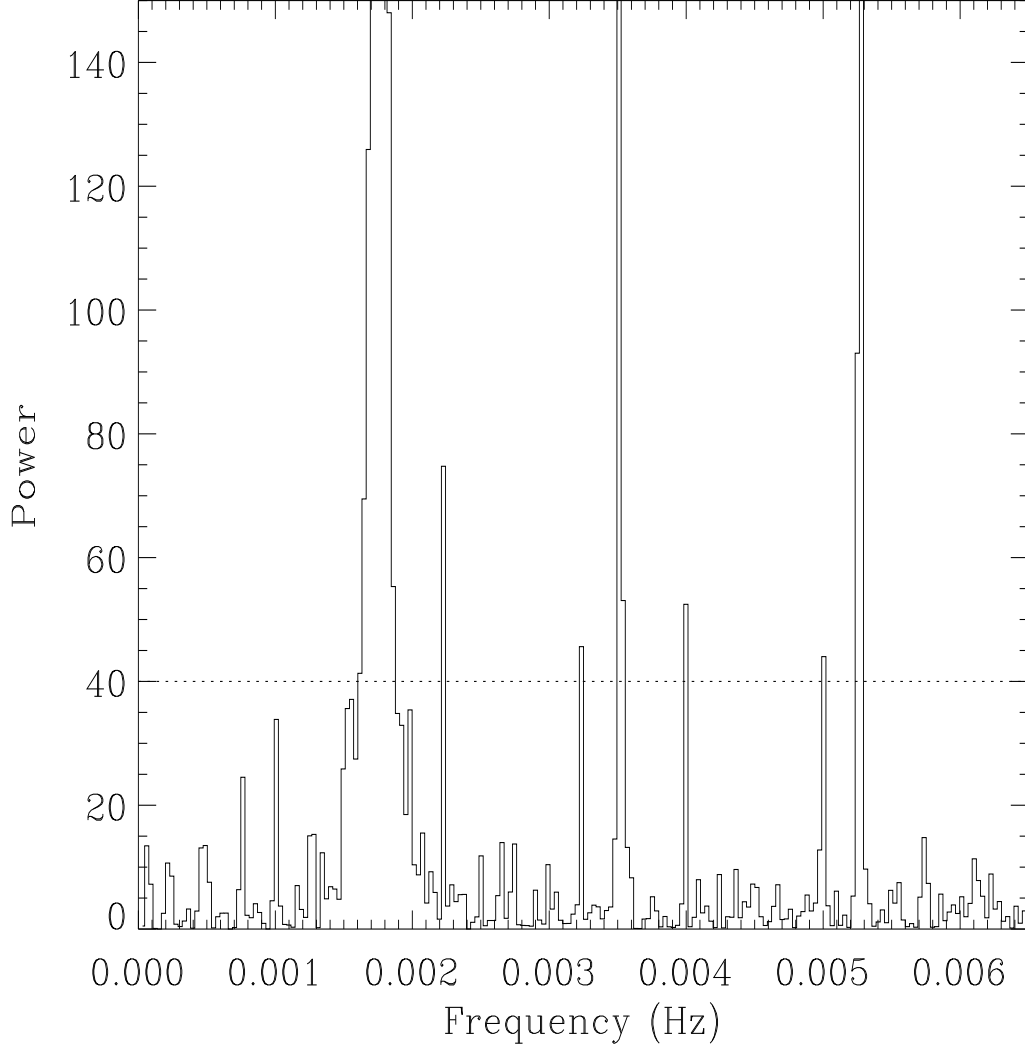


Figure 10: Low frequency power spectrum of our longest *Chandra* pointing. The power spectrum is normalized such that a pure poisson noise process would have a mean of 2 and be distributed as χ^2 with two degrees of freedom. The three peaks that go off-scale are the fundamental, first and second harmonic of the 1.756 mHz modulation. Upper sidebands to the fundamental and first harmonic, and lower sidebands to the first and second harmonics are present. The horizontal dotted line indicates the power level with a single trial chance probability of $\approx 2 \times 10^{-9}$. We suspect the sidebands are an artifact introduced by the *Chandra* dither (see the text for a detailed discussion).

Table 1: *Chandra* Observations of V407 Vul

	OBSID	Instrument	Start UTC	Stop UTC	Exp (ksec)
1	300095	ACIS-S (CC-mode)	Feb 18, 2003:11:16:30	Feb 18, 2003:15:23:39	13.4
2	300095	ACIS-S (CC-mode)	Feb 19, 2003:07:49:17	Feb 19, 2003:17:58:49	35.4
3	300096	ACIS-S (CC-mode)	Nov 11, 2003:19:33:05	Nov 11, 2003:23:06:22	11.2
4	300111	ACIS-S (CC-mode)	Dec 27, 2003:02:36:24	Dec 27, 2003:07:30:14	15.4
5	300112	ACIS-S (CC-mode)	Jan 31, 2004:21:20:12	Feb 01, 2004:02:05:30	15.1

Table 2: Timing Solution for V407 Vul

Model Parameter	Value
t_0 (TDB)	MJD 49257.533373137
ν_0 (Hz)	0.0017562462(2)
$\dot{\nu}$ (Hz s ⁻¹)	$7.0(8) \times 10^{-18}$